COMPUTER METHODS IN APPLIED MECHANICS AND ENGINEERING 74 (1989) 307–326
NORTH-HOLLAND

NUMERICAL ANALYSIS OF JUNCTIONS BETWEEN PLATES

Michel BERNADOU, Séverine FAYOLLE
INRIA, Rocquencourt, 78153 Le Chesnay, France

Françoise LÉNÉ
Laboratoire d'Acoustique et Mécanique (U.A. 868 du CNRS), Université Pierre et Marie Curie, 75252 Paris Cedex 05, France
and
INRIA, Rocquencourt, 78153 Le Chesnay, France

Received 15 December 1988

The junctions of bars, plates and shells are the basic ingredients of any industrial structural construction. The numerical simulation of such junctions is a classical part of the commercial finite element codes.

On the other hand there seem to be very few mathematical studies of such junctions. In this paper, we propose a variational formulation of plate junctions when these junctions can be considered as elastic or rigid hinges. Then, we study the mathematical properties of these equations as their appoximation by finite element methods. We conclude by reporting some numerical experiments.

1. Introduction

Many industrial constructions use, as basic components, elastic solids, bars, plates and shells. The numerical simulation of such assemblages needs a good approximation of each constitutive element as well as a good representation of their junctions. In engineering literature, there are many contributions on the best way to modelize and, particularly, to compute such constructions. Thus, for the modelization of the mechanical engineering aspects, we refer the reader to [1, chapter 6], which is devoted to multishell structures, while for finite element methods we can recommand [2, 3] and their references.

By contrast there are very few mathematical studies in these directions. We mention some recent works, [4, 6], which are mainly concerned with the problem of the junction between three-dimensional and two-dimensional linearly elastic structures, while [7, 8] consider asymptotic developments for junction of two plates.

In this paper we restrict our attention to the numerical analysis of the junction between two plates. Our study is based on the following assumptions:
—small deformations,
—elastic, homogeneous, isotropic material,
—deformation through the thickness obeys the Kirchhoff–Love hypothesis,
—the junction can be assimilated to a rigid or an elastic hinge.

The contents of this paper can be outlined as follows. Section 2 discusses the mechanical

0045-7825/89/$3.50

modelling of the junction of plates in terms of partial differential equations. We start by recalling the general Kirchhoff–Love plate equations and then we introduce the modellization of the junction as an elastic or a rigid hinge. Section 3 gives the variational formulations of these different junctions and the corresponding existence results. It is also proved that the elastic hinge becomes rigid when its stiffness becomes infinite. Section 4 contains the approximation by conforming finite element methods and Section 5 presents some numerical examples.

2. Mechanical Modelling

In this paragraph we introduce the main notations and the basic equations that we will use subsequently.

2.1. Hypotheses and notations

In this section we will recall the equations of only one thin plate. Let $\mathscr{E}^3$ be the Euclidean space referred to the orthonormal system $(0, \boldsymbol{e}_1, \boldsymbol{e}_2, \boldsymbol{e}_3)$. Consider a plate whose middle surface lies in the plane $(0, \boldsymbol{e}_1, \boldsymbol{e}_2)$ and coincides with the domain $S \subset \mathbb{R}^2$. We assume that the boundary ∂S of S is sufficiently smooth.

Classically, the displacement field of the current point $P(x_1, x_2, x_3)$ of the plate can be described by

$$U(x_1, x_2, x_3) = [u_\alpha(x_1, x_2) + x_3 l_\alpha(x_1, x_2)]\boldsymbol{e}_\alpha + u_3(x_1, x_2)\boldsymbol{e}_3 , \tag{2.1.1}$$

where

$$\boldsymbol{l} = \boldsymbol{\Omega} \times \boldsymbol{e}_3 , \tag{2.1.2}$$

$\boldsymbol{\Omega}$ denoting the inifinitesimal rotation vector.

In (2.1.1) and further, we use the summation convention on repeated indices. Latin indices $i, j, \ldots$ take their values in the set $\{1, 2, 3\}$ while greek indices $\alpha, \beta, \ldots$ take their values in the set $\{1, 2\}$.

Then, the strain tensor is given by its components upon the basis $(\boldsymbol{e}_1, \boldsymbol{e}_2, \boldsymbol{e}_3)$:

$$D_{\alpha\beta} = e_{\alpha\beta} + x_3 K_{\alpha\beta} , \qquad 2D_{\alpha 3} = l_\alpha + u_{3,\alpha} , \qquad D_{33} = 0 , \tag{2.1.3}$$

where

$$2e_{\alpha\beta}(\boldsymbol{u}) = u_{\alpha,\beta} + u_{\beta,\alpha} , \qquad 2K_{\alpha\beta} = l_{\alpha,\beta} + l_{\beta,\alpha} . \tag{2.1.4}$$

By using the Kirchhoff–Love assumption ($D_{\alpha 3} = 0$), we obtain that the nonzero components of the strain field are determined by (2.1.3) from the knowledge of both symmetric tensor fields $e_{\alpha\beta}$ and $K_{\alpha\beta}$. They can be expressed as functions of the components of the middle surface displacement as follows:

$$2e_{\alpha\beta}(\boldsymbol{u}) = u_{\alpha,\beta} + u_{\beta,\alpha} , \qquad K_{\alpha\beta}(\boldsymbol{u}) = -u_{3,\alpha\beta} . \tag{2.1.5}$$

According to [9], the internal loads associated to the considered kinematics, are described by

(i) a symmetrical tensor of stress resultants $N_{\alpha\beta}$,
(ii) a symmetrical tensor of stress couples $M_{\alpha\beta}$.

We assume that the external loads induce

(i) a distribution of forces whose resultant is $\boldsymbol{p} = p_i \boldsymbol{e}_i$ on the middle surface S and whose resultant moment is $\boldsymbol{0}$ on S,

(ii) a distribution of forces whose resultant is $\boldsymbol{T} = T_i \boldsymbol{e}_i$ on ∂S and whose resultant moment is $\boldsymbol{\mathcal{M}} = \mathcal{M}_n \boldsymbol{n} + \mathcal{M}_t \boldsymbol{t}$, where $\boldsymbol{n}$ denotes the unit external normal to ∂S in the plane of S and where $\boldsymbol{t} = \boldsymbol{e}_3 \times \boldsymbol{n}$.

The equilibrium equations, obtained by the principle of virtual work, can be written as follows:

$$N_{\alpha\beta,\beta} + p_\alpha = 0 \quad \text{in } S\,, \tag{2.1.6}$$

$$M_{\alpha\beta,\alpha\beta} + p_3 = 0 \quad \text{in } S\,, \tag{2.1.7}$$

with the boundary conditions

$$T_3 - \mathcal{M}_{n,t} = M_{\alpha\beta,\beta} n_\alpha + (M_{\alpha\beta} n_\beta t_\alpha)_{,t} \quad \text{on } \partial S\,, \tag{2.1.8}$$

$$T_\alpha = N_{\alpha\beta} n_\beta \quad \text{on } \partial S\,, \tag{2.1.9}$$

$$\mathcal{M}_t = M_{\alpha\beta} n_\alpha n_\beta \quad \text{on } \partial S\,, \tag{2.1.10}$$

where n_α and t_α are the components of vectors $\boldsymbol{n}$ and $\boldsymbol{t}$, i.e., $\boldsymbol{n} = n_\alpha \boldsymbol{e}_\alpha$, $\boldsymbol{t} = t_\alpha \boldsymbol{e}_\alpha$.

Finally, the deformations are assumed to be small and governed by the equations of the linear elasticity, and the material is supposed to be homogeneous and isotropic. Then, the behaviour law of the plate is described by (see [9]):

$$N_{\alpha\beta} = \frac{Ee}{1-\nu^2}\,((1-\nu)e_{\alpha\beta} + \nu e_{\gamma\gamma}\delta_{\alpha\beta})\,, \tag{2.1.11}$$

$$M_{\alpha\beta} = \frac{Ee^3}{12(1-\nu^2)}\,((1-\nu)K_{\alpha\beta} + \nu K_{\gamma\gamma}\delta_{\alpha\beta})\,, \tag{2.1.12}$$

where e, E and ν denote the thickness of the plate, the Young modulus and the Poisson coefficient of the material, respectively.

2.2. Junction of two plates

Consider two plates with distinct middle surfaces S and $\underset{\sim}{S}$ which join along a common rectilinear boundary Γ (see Fig. 1). From now on, we denote by $(\cdot)$ the quantities related to the plate S, while $(\underset{\sim}{\ })$ denotes the quantities related to the plate $\underset{\sim}{S}$.

Upon the boundaries ∂S and $\partial \underset{\sim}{S}$, we define two local direct orthonormal reference systems $(\boldsymbol{n}, \boldsymbol{t}, \boldsymbol{e}_3)$ and $(\underset{\sim}{\boldsymbol{n}}, \underset{\sim}{\boldsymbol{t}}, \underset{\sim}{\boldsymbol{e}}_3)$ which include as intrinsic vectors the unit external normals $\boldsymbol{n}$ and $\underset{\sim}{\boldsymbol{n}}$ to

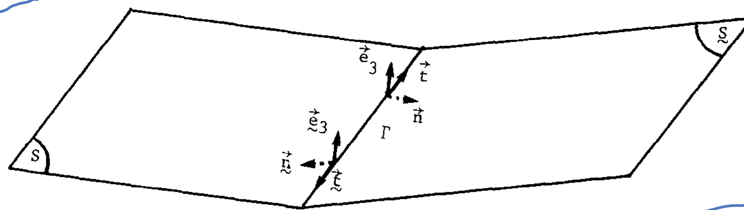

Fig. 1. Junction of two plates.

the boundaries ∂S and $\partial \underset{\sim}{S}$ in the planes respectively determined by S and $\underset{\sim}{S}$. If we define

$$\underset{\sim}{\boldsymbol{t}} = -\boldsymbol{t} \quad \text{and} \quad \underset{\sim}{\boldsymbol{e}}_3 = \underset{\sim}{\boldsymbol{n}} \times \underset{\sim}{\boldsymbol{t}}\,, \tag{2.2.1}$$

then both lines ∂S and $\partial \underset{\sim}{S}$ are positively oriented with respect to $\boldsymbol{e}_3$ and $\underset{\sim}{\boldsymbol{e}}_3$.

Finally, we define the angle θ between both plates, with respect to the reference system $(\boldsymbol{n}, \boldsymbol{t}, \boldsymbol{e}_3)$ attached to the common side Γ:

$$\theta = (\boldsymbol{n}, \underset{\sim}{\boldsymbol{n}})_t\,. \tag{2.2.2}$$

In particular, when both plates are coplanar and placed side by side, this angle is equal to π while this angle is equal to 0 when the plates are superposed. All these geometrical considerations are illustrated in Fig. 1.

For any behaviour of the hinge Γ, the application of the action–reaction principle at any point of Γ implies the transmission of the efforts, i.e.,

$$\boldsymbol{T}(M) = \underset{\sim}{\boldsymbol{T}}(M) \quad \text{and} \quad \boldsymbol{\mathcal{M}}(M) = \underset{\sim}{\boldsymbol{\mathcal{M}}}(M) \quad \forall M \in \Gamma\,. \tag{2.2.3}$$

In particular, note that $\boldsymbol{\mathcal{M}}(M) = \underset{\sim}{\boldsymbol{\mathcal{M}}}(M)$ on Γ implies $\mathcal{M}_n(M) = \underset{\sim}{\mathcal{M}}_{\underset{\sim}{n}}(M) = 0\ \forall M \in \Gamma$, so that $\boldsymbol{\mathcal{M}}(M) = \underset{\sim}{\boldsymbol{\mathcal{M}}}(M) = \mathcal{M}_t(M)\boldsymbol{t}\ \forall M \in \Gamma$.

Subsequently, we examine two types of behaviours:

(i) a rigid behaviour for which the continuity of the displacements and of the rotations is insured at any point M of Γ, i.e.,

$$\boldsymbol{u}(M) = \underset{\sim}{\boldsymbol{u}}(M)\,, \qquad \boldsymbol{\Omega}(M) \cdot \boldsymbol{t} = \underset{\sim}{\boldsymbol{\Omega}}(M) \cdot \boldsymbol{t}\,, \tag{2.2.4}$$

where $\boldsymbol{\Omega}$ (resp. $\underset{\sim}{\boldsymbol{\Omega}}$) is defined by relation (2.1.2)

(ii) an elastic behaviour for which only the continuity of the displacements is insured at any point M of Γ, i.e.,

$$\boldsymbol{u}(M) = \underset{\sim}{\boldsymbol{u}}(M)\,, \qquad \mathcal{M}_t(M) = -k[\boldsymbol{\Omega}(M) - \underset{\sim}{\boldsymbol{\Omega}}(M)] \cdot \boldsymbol{t}\,. \tag{2.2.5}$$

Thus, the second equation of relation (2.2.4) is replaced by the requirement that the moment $\boldsymbol{\mathcal{M}}$ is proportional to the jump of the tangential components of rotations along the hinge Γ. The coefficient k of elastic stiffness of the hinge is a given positive number attached to the problem into consideration.

Junction conditions in terms of displacement components

Let us consider the junction conditions (2.2.4) and (2.2.5) which are expressed in vectorial forms. By using the components of displacements and rotations upon the above reference systems, we are able to get the expression of the junction conditions in terms of components. At any point $M \in \Gamma$, let us set

$$\boldsymbol{u}(M) = u_n \boldsymbol{n} + u_t \boldsymbol{t} + u_3 \boldsymbol{e}_3 \,, \qquad \underset{\sim}{\boldsymbol{u}}(M) = \underset{\sim}{u}_{\underset{\sim}{n}} \underset{\sim}{\boldsymbol{n}} + \underset{\sim}{u}_{\underset{\sim}{t}} \underset{\sim}{\boldsymbol{t}} + \underset{\sim}{u}_3 \underset{\sim}{\boldsymbol{e}}_3 \,. \tag{2.2.6}$$

Definitions (2.2.1) and (2.2.2) imply

$$\boldsymbol{n} = \underset{\sim}{\boldsymbol{n}} \cos\theta - \underset{\sim}{\boldsymbol{e}}_3 \sin\theta \,, \qquad \boldsymbol{t} = -\underset{\sim}{\boldsymbol{t}} \,, \qquad \boldsymbol{e}_3 = -\underset{\sim}{\boldsymbol{n}} \sin\theta - \underset{\sim}{\boldsymbol{e}}_3 \cos\theta \,,$$

so that, using (2.2.6),

$$\underset{\sim}{u}_{\underset{\sim}{n}} = u_n \cos\theta - u_3 \sin\theta \,, \qquad \underset{\sim}{u}_{\underset{\sim}{t}} = -u_t \,, \qquad \underset{\sim}{u}_3 = -u_n \sin\theta - u_3 \cos\theta \,. \tag{2.2.7}$$

On the other hand, the assumption $D_{\alpha 3} = 0$ involves $l_\alpha = -u_{3,\alpha}$ or, equivalently, $l_t = -u_{3,t}$ and $l_n = -u_{3,n}$. By setting

$$\boldsymbol{\Omega} = \Omega_n \boldsymbol{n} + \Omega_t \boldsymbol{t} + \Omega_3 \boldsymbol{e}_3 \,,$$

the equation $\boldsymbol{l} = \boldsymbol{\Omega} \times \boldsymbol{e}_3 = -\Omega_n \boldsymbol{t} + \Omega_t \boldsymbol{n}$ implies $\Omega_n = -l_t = u_{3,t}$, $\Omega_t = l_n = -u_{3,n}$, so that

$$\boldsymbol{\Omega}(M) = u_{3,t} \boldsymbol{n} - u_{3,n} \boldsymbol{t} + \Omega_3 \boldsymbol{e}_3 \quad \forall M \in \Gamma \,. \tag{2.2.8}$$

Similarly,

$$\underset{\sim}{\boldsymbol{\Omega}}(M) = \underset{\sim}{u}_{3,\underset{\sim}{t}} \underset{\sim}{\boldsymbol{n}} - \underset{\sim}{u}_{3,\underset{\sim}{n}} \underset{\sim}{\boldsymbol{t}} + \underset{\sim}{\Omega}_3 \underset{\sim}{\boldsymbol{e}}_3 \quad \forall M \in \Gamma \,.$$

so that the relation $\underset{\sim}{\boldsymbol{t}} = -\boldsymbol{t}$ implies

$$\boldsymbol{\Omega}(M) - \underset{\sim}{\boldsymbol{\Omega}}(M) = -(u_{3,n} + \underset{\sim}{u}_{3,\underset{\sim}{n}}) \boldsymbol{t} + u_{3,t} \boldsymbol{n} - \underset{\sim}{u}_{3,\underset{\sim}{t}} \underset{\sim}{\boldsymbol{n}} + \Omega_3 \boldsymbol{e}_3 - \underset{\sim}{\Omega}_3 \underset{\sim}{\boldsymbol{e}}_3 \,. \tag{2.2.9}$$

Thus, by assuming that we have a 'real' junction ($\theta \neq k\pi$, $k \in \mathbb{Z}$), the vectors $(\boldsymbol{n}, \boldsymbol{t}, \underset{\sim}{\boldsymbol{n}})$ are independent. Then we have the following cases to consider:

(i) Rigid hinge: From (2.2.9), condition $\boldsymbol{\Omega}(M) \cdot \boldsymbol{t} = \underset{\sim}{\boldsymbol{\Omega}}(M) \cdot \boldsymbol{t}$ implies

$$u_{3,n} + \underset{\sim}{u}_{3,\underset{\sim}{n}} = 0 \quad \text{on } \Gamma \,, \tag{2.2.10}$$

(ii) Elastic hinge: Relations (2.2.5) and (2.2.9) imply

$$k(u_{3,n} + \underset{\sim}{u}_{3,\underset{\sim}{n}}) = \mathcal{M}_t(M) \quad \text{on } \Gamma \,. \tag{2.2.11}$$

REMARK 2.2.1. The rigid behaviour can be interpretated as the limit case ($k \to \infty$) of the elastic behaviour of a hinge whose stiffness coefficient would be very large. We will return to this result in Section 3.3.

2.3. The equations of the junction problem

In Section 2.1 we have recalled the equations of a plate, while, in Section 2.2, we have obtained the junction conditions of two plates both for rigid or elastic hinges, in vectorial forms and in terms of components.

For simplicity, we further assume that the plate S is clamped on a part ∂S_0 of its boundary, with measure $(\partial S_0) > 0$, so that

$$\boldsymbol{u} = \boldsymbol{0}\,, \quad u_{3,n} = 0 \quad \text{on } \partial S_0\,.$$

The complementary part of the boundary ∂S is assumed to be such that

$$\partial S - \partial S_0 = \Gamma \cup \partial S_1\,, \tag{2.3.1}$$

where $\Gamma = \partial S \cap \partial \underset{\sim}{S}$ and where ∂S_1 is loaded by $(\boldsymbol{T}, \boldsymbol{\mathcal{M}})$. Likewise, we assume that

$$\partial \underset{\sim}{S}_0 = \emptyset \text{ (not essential)}\,, \qquad \partial \underset{\sim}{S} = \Gamma \cup \partial \underset{\sim}{S}_1\,, \tag{2.3.2}$$

where $\partial \underset{\sim}{S}_1$ is loaded by $(\underset{\sim}{\boldsymbol{T}}, \underset{\sim}{\boldsymbol{\mathcal{M}}})$.

Then, by assembling all the previous results, the equations of this junction problem of plates are

$$N_{\alpha\beta,\beta} + p_\alpha = 0\,, \quad M_{\alpha\beta,\alpha\beta} + p_3 = 0 \quad \text{in } S\,, \tag{2.3.3}$$

$$\underset{\sim}{N}_{\alpha\beta,\beta} + \underset{\sim}{p}_\alpha = 0\,, \quad \underset{\sim}{M}_{\alpha\beta,\alpha\beta} + \underset{\sim}{p}_3 = 0 \quad \text{in } \underset{\sim}{S}\,, \tag{2.3.4}$$

$$\boldsymbol{u} = \boldsymbol{0}\,, \quad u_{3,n} = 0 \qquad \text{on } \partial S_0\,, \tag{2.3.5}$$

$$T_3 - \mathcal{M}_{n,t} = M_{\alpha\beta,\beta} n_\alpha + (M_{\alpha\beta} n_\beta t_\alpha)_{,t}\,, \quad T_\alpha = N_{\alpha\beta} n_\beta\,, \quad \mathcal{M}_t = M_{\alpha\beta} n_\alpha n_\beta \quad \text{on } \partial S_1\,, \tag{2.3.6}$$

$$\underset{\sim}{T}_3 - \underset{\sim}{\mathcal{M}}_{\underset{\sim}{n},\underset{\sim}{t}} = \underset{\sim}{M}_{\alpha\beta,\beta} \underset{\sim}{n}_\alpha + (\underset{\sim}{M}_{\alpha\beta} \underset{\sim}{n}_\beta \underset{\sim}{t}_\alpha)_{,\underset{\sim}{t}}\,, \quad \underset{\sim}{T}_\alpha = \underset{\sim}{N}_{\alpha\beta} \underset{\sim}{n}_\beta\,, \quad \underset{\sim}{\mathcal{M}}_{\underset{\sim}{t}} = \underset{\sim}{M}_{\alpha\beta} \underset{\sim}{n}_\alpha \underset{\sim}{n}_\beta \quad \text{on } \partial \underset{\sim}{S}_1\,, \tag{2.3.7}$$

and the conditions of junction upon Γ which are depending on the type of hinge are

$$\left.\begin{aligned} &\boldsymbol{u} = \underset{\sim}{\boldsymbol{u}} && \text{on } \Gamma\,, && (2.3.8)\\ &u_{3,n} + \underset{\sim}{u}_{3,\underset{\sim}{n}} = 0 && \text{on } \Gamma\,, && (2.3.9)\end{aligned}\right\}\ \text{(rigid hinge)}$$

$$\left.\begin{aligned} &\boldsymbol{u} = \underset{\sim}{\boldsymbol{u}} && \text{on } \Gamma && (2.3.10)\\ &k(u_{3,n} + \underset{\sim}{u}_{3,\underset{\sim}{n}}) = \mathcal{M}_t(M) && \text{on } \Gamma && (2.3.11)\end{aligned}\right\}\ \text{(elastic hinge)}$$

3. Variational formulations and existence results

From the equations stated in Section 2.3, we derive the corresponding variational formulations in suitable spaces, and then we prove existence and uniqueness results. We conclude by examining the behaviour of the elastic hinge when $k \to +\infty$.

3.1. The case of an elastic hinge

Let us consider the first plate S independently of a possible junction with another plate $\underset{\sim}{S}$. By multiplying the equilibrium equations (2.1.6) and (2.1.7) by test functions v_α and v_3, by integrating by parts upon the middle surface S and then, by taking into account the general boundary conditions (2.1.8)–(2.1.10), we obtain with (2.1.5):

$$\int_S (N_{\alpha\beta} e_{\alpha\beta}(\boldsymbol{v}) + M_{\alpha\beta} K_{\alpha\beta}(\boldsymbol{v}))\, \mathrm{d}S = \int_S \boldsymbol{p} \cdot \boldsymbol{v}\, \mathrm{d}S + \int_{\partial S} (\boldsymbol{T} \cdot \boldsymbol{v} + \mathcal{M}_n v_{3,t} - \mathcal{M}_t v_{3,n})\, \mathrm{d}s\,. \tag{3.1.1}$$

Exactly in the same way, we would get for the plate $\underset{\sim}{S}$

$$\int_{\underset{\sim}{S}} (\underset{\sim}{N}_{\alpha\beta} \underset{\sim}{e}_{\alpha\beta}(\underset{\sim}{\boldsymbol{v}}) + \underset{\sim}{M}_{\alpha\beta} \underset{\sim}{K}_{\alpha\beta}(\underset{\sim}{\boldsymbol{v}}))\, \mathrm{d}\underset{\sim}{S} = \int_{\underset{\sim}{S}} \underset{\sim}{\boldsymbol{p}} \cdot \underset{\sim}{\boldsymbol{v}}\, \mathrm{d}\underset{\sim}{S} + \int_{\partial \underset{\sim}{S}} (\underset{\sim}{\boldsymbol{T}} \cdot \underset{\sim}{\boldsymbol{v}} + \underset{\sim}{\mathcal{M}}_{\underset{\sim}{n}} \underset{\sim}{v}_{3,\underset{\sim}{t}} - \underset{\sim}{\mathcal{M}}_{\underset{\sim}{t}} \underset{\sim}{v}_{3,\underset{\sim}{n}})\, \mathrm{d}\underset{\sim}{s}\,. \tag{3.1.2}$$

Now we assume that both plates S and $\underset{\sim}{S}$ are such that

(i) the plate S is clamped along ∂S_0, i.e., the conditions (2.3.5) are satisfied,

(ii) the plates S and $\underset{\sim}{S}$ are joining along the common side Γ so that conditions (2.3.8), (2.3.9), or (2.3.10), (2.3.11) are satisfied, depending on the type of hinge we are considering.

With notations (2.3.1) and (2.3.2) we obtain, by adding (3.1.1) and (3.1.2),

$$\begin{aligned}
&\int_S (N_{\alpha\beta} e_{\alpha\beta}(\boldsymbol{v}) + M_{\alpha\beta} K_{\alpha\beta}(\boldsymbol{v}))\, \mathrm{d}S + \int_{\underset{\sim}{S}} (\underset{\sim}{N}_{\alpha\beta} \underset{\sim}{e}_{\alpha\beta}(\underset{\sim}{\boldsymbol{v}}) + \underset{\sim}{M}_{\alpha\beta} \underset{\sim}{K}_{\alpha\beta}(\underset{\sim}{\boldsymbol{v}}))\, \mathrm{d}\underset{\sim}{S} \\
&= \int_S \boldsymbol{p} \cdot \boldsymbol{v}\, \mathrm{d}S + \int_{\underset{\sim}{S}} \underset{\sim}{\boldsymbol{p}} \cdot \underset{\sim}{\boldsymbol{v}}\, \mathrm{d}\underset{\sim}{S} + \int_{\partial S_1} \{\boldsymbol{T} \cdot \boldsymbol{v} + \mathcal{M}_n v_{3,t} - \mathcal{M}_t v_{3,n}\}\, \mathrm{d}s \\
&\quad + \int_{\partial \underset{\sim}{S}_1} \{\underset{\sim}{\boldsymbol{T}} \cdot \underset{\sim}{\boldsymbol{v}} + \underset{\sim}{\mathcal{M}}_{\underset{\sim}{n}} \underset{\sim}{v}_{3,\underset{\sim}{t}} - \underset{\sim}{\mathcal{M}}_{\underset{\sim}{t}} \underset{\sim}{v}_{3,\underset{\sim}{n}}\}\, \mathrm{d}\underset{\sim}{s} + \int_\Gamma \{\boldsymbol{T} \cdot (\boldsymbol{v} - \underset{\sim}{\boldsymbol{v}}) - \mathcal{M}_t (v_{3,n} + \underset{\sim}{v}_{3,\underset{\sim}{n}})\}\, \mathrm{d}\gamma\,.
\end{aligned} \tag{3.1.3}$$

To express the last integral we have used properties (2.2.3) of transmission of the efforts, i.e., $\boldsymbol{T} = \underset{\sim}{\boldsymbol{T}}$ on Γ and $\boldsymbol{\mathcal{M}} = \underset{\sim}{\boldsymbol{\mathcal{M}}}$ on Γ, that is equivalent to $\mathcal{M}_t = -\underset{\sim}{\mathcal{M}}_{\underset{\sim}{t}}$, $\mathcal{M}_n = 0$ and $\underset{\sim}{\mathcal{M}}_{\underset{\sim}{n}} = 0$ along Γ.

Let us emphasize that (3.1.3) is valid for rigid hinge as well as for elastic hinge. Now let us specialize (3.1.3) to the case of an elastic hinge. In order to set up the variational formulation of the problem we must

(i) substitute the behaviour laws (2.1.11) and (2.1.12) (and similar relations for plate $\underset{\sim}{S}$) into (3.1.3),

(ii) define a suitable admissible displacement space. In this way, we set

$$
\begin{aligned}
&V_1 = \{v \in H^1(S) \mid v = 0 \text{ on } \partial S_0\}\,, \\
&V_2 = \{v \in H^2(S) \mid v = v_{,n} = 0 \text{ on } \partial S_0\}\,, \qquad (3.1.4)\\
&V = V_1 \times V_1 \times V_2\,,
\end{aligned}
$$

and

$$
\utilde{V} = H^1(\utilde{S}) \times H^1(\utilde{S}) \times H^2(\utilde{S})\,, \qquad (3.1.5)
$$

so that the kinematically admissible displacement field for an elastic junction problem is

$$
W_{\mathrm{El}} = \{(w;\utilde{w}) \in V \times \utilde{V} \mid w = \utilde{w} \text{ on } \Gamma\}\,, \qquad (3.1.6)
$$

(iii) substitute (2.3.11) into (3.1.3).

Then, the variational formulation of the problem can be stated as follows:

$$
\begin{aligned}
&\text{Find } (u;\utilde{u}) \in W_{\mathrm{El}}\,, \quad \text{such that } a[(u;\utilde{u}),(v;\utilde{v})] + kb[(u;\utilde{u}),(v;\utilde{v})] = l(v;\utilde{v}) \\
&\qquad\qquad\qquad\qquad\quad \forall (v;\utilde{v}) \in W_{\mathrm{El}}\,, \qquad (3.1.7)
\end{aligned}
$$

where

$$
\begin{aligned}
a[(u;\utilde{u}),(v;\utilde{v})] = {} & \int_S \frac{Ee}{1-\nu^2}\,((1-\nu)e_{\alpha\beta}(u)e_{\alpha\beta}(v) + \nu e_{\alpha\alpha}(u)e_{\beta\beta}(v))dS \\
& + \int_S \frac{Ee^3}{12(1-\nu^2)}\,((1-\nu)K_{\alpha\beta}(u)K_{\alpha\beta}(v) + \nu K_{\alpha\alpha}(u)K_{\beta\beta}(v))\,\mathrm{d}S \\
& + \int_{\utilde{S}} \frac{\utilde{E}\utilde{e}}{1-\utilde{\nu}^2}\,((1-\utilde{\nu})\utilde{e}_{\alpha\beta}(\utilde{u})\utilde{e}_{\alpha\beta}(\utilde{v}) + \utilde{\nu}\utilde{e}_{\alpha\alpha}(\utilde{u})\utilde{e}_{\beta\beta}(\utilde{v}))\,\mathrm{d}\utilde{S} \\
& + \int_{\utilde{S}} \frac{\utilde{E}\utilde{e}^3}{12(1-\utilde{\nu}^2)}\,((1-\utilde{\nu})\utilde{K}_{\alpha\beta}(\utilde{u})\utilde{K}_{\alpha\beta}(\utilde{v}) + \utilde{\nu}\utilde{K}_{\alpha\alpha}(\utilde{u})\utilde{K}_{\beta\beta}(\utilde{v}))\,\mathrm{d}\utilde{S}\,,
\end{aligned}
$$

(3.1.8)

$$
b[(u;\utilde{u}),(v;\utilde{v})] = \int_\Gamma (u_{3,n} + \utilde{u}_{3,\utilde{n}})(v_{3,n} + \utilde{v}_{3,\utilde{n}})\,\mathrm{d}\gamma\,, \qquad (3.1.9)
$$

$$
\begin{aligned}
l(v;\utilde{v}) = {} & \int_S p\cdot v\,\mathrm{d}S + \int_{\utilde{S}} \utilde{p}\cdot\utilde{v}\,\mathrm{d}\utilde{S} + \int_{\partial S_1} (T\cdot v + \mathcal{M}_n v_{3,t} - \mathcal{M}_t v_{3,n})\,\mathrm{d}s \\
& + \int_{\partial\utilde{S}_1} (\utilde{T}\cdot\utilde{v} + \utilde{\mathcal{M}}_{\utilde{n}}\utilde{v}_{3,\utilde{t}} - \utilde{\mathcal{M}}_{\utilde{t}}\utilde{v}_{3,\utilde{n}})\,\mathrm{d}\utilde{s}\,. \qquad (3.1.10)
\end{aligned}
$$

Thus, we obtain the following theorem:

THEOREM 3.1.1. Assume that

$$\begin{aligned}
&\boldsymbol{p}\in(L^2(S))^3\,, \quad \boldsymbol{T}\in(L^2(\partial S_1))^3\,, \quad \mathcal{M}_n\in L^2(\partial S_1)\,, \quad \mathcal{M}_t\in L^2(\partial S_1)\,,\\
&\underset{\sim}{\boldsymbol{p}}\in(L^2(\underset{\sim}{S}))^3\,, \quad \underset{\sim}{\boldsymbol{T}}\in(L^2(\partial \underset{\sim}{S}_1))^3\,, \quad \underset{\sim}{\mathcal{M}}_{\underset{\sim}{n}}\in L^2(\partial \underset{\sim}{S}_1)\,, \quad \underset{\sim}{\mathcal{M}}_{\underset{\sim}{t}}\in L^2(\partial \underset{\sim}{S}_1)\,,\\
&k>0\,, \quad E>0\,, \quad \underset{\sim}{E}>0\,, \quad 0<\nu<\tfrac12\,, \quad 0<\underset{\sim}{\nu}<\tfrac12\,.
\end{aligned} \tag{3.1.11}$$

Then, (3.1.7) has one and only one solution.

PROOF. We give the main lines of this proof and we refer to [10] for more details. It takes three steps.

Step 1. The space W_{El}, defined by (3.1.6), is a closed subspace of the space

$$E=[H^1(S)]^2\times H^2(S)\times[H^1(\underset{\sim}{S})]^2\times H^2(\underset{\sim}{S})\,, \tag{3.1.12}$$

equipped with the norm

$$\begin{aligned}
\|(\boldsymbol{v};\underset{\sim}{\boldsymbol{v}})\|_E=(&\|v_1\|^2_{H^1(S)}+\|v_2\|^2_{H^1(S)}+\|v_3\|^2_{H^2(S)}+\|\underset{\sim}{v}_1\|^2_{H^1(\underset{\sim}{S})}+\|\underset{\sim}{v}_2\|^2_{H^1(\underset{\sim}{S})}\\
&+\|\underset{\sim}{v}_3\|^2_{H^2(\underset{\sim}{S})})^{1/2}\,.
\end{aligned} \tag{3.1.13}$$

Step 2. In the space W_{El}, the functional

$$\begin{aligned}
|(\boldsymbol{v};\underset{\sim}{\boldsymbol{v}})|_{W_{\mathrm{El}}}=\Big(&\int_S[e_{\alpha\beta}(\boldsymbol{v})e_{\alpha\beta}(\boldsymbol{v})+K_{\alpha\beta}(\boldsymbol{v})K_{\alpha\beta}(\boldsymbol{v})]\,\mathrm{d}S\\
&+\int_{\underset{\sim}{S}}[\underset{\sim}{e}_{\alpha\beta}(\underset{\sim}{\boldsymbol{v}})\underset{\sim}{e}_{\alpha\beta}(\underset{\sim}{\boldsymbol{v}})+\underset{\sim}{K}_{\alpha\beta}(\underset{\sim}{\boldsymbol{v}})\underset{\sim}{K}_{\alpha\beta}(\underset{\sim}{\boldsymbol{v}})]\,\mathrm{d}\underset{\sim}{S}+b[(\boldsymbol{v};\underset{\sim}{\boldsymbol{v}}),(\boldsymbol{v};\underset{\sim}{\boldsymbol{v}})]\Big)^{1/2}
\end{aligned}$$

is a norm equivalent to the usual norm (3.1.13).

Step 3. From Step 2, we deduce the W_{El}-ellipticity of the bilinear form

$$a[(\cdot\,;\cdot),(\cdot\,;\cdot)]+kb(\cdot\,;\cdot),(\cdot\,;\cdot)]$$

for any constant $k>0$. To conclude, it remains to apply the Lax–Milgran lemma. □

REMARK 3.1.1. The assumption $k=\text{constant}>0$ is not essential. One can assume that k is a smooth function of the arc length x along Γ with $k(x)>0$.

3.2. The case of a rigid hinge

By taking into account the junction conditions (2.3.8), (2.3.9) of the hinge, the space of the kinematically admissible fields is now

$$W_{\mathrm{Rig}}=\{(\boldsymbol{w};\underset{\sim}{\boldsymbol{w}})\in V\times\underset{\sim}{V}\mid \boldsymbol{w}=\underset{\sim}{\boldsymbol{w}}\ \text{on}\ \Gamma\,,\ w_{3,n}+\underset{\sim}{w}_{3,\underset{\sim}{n}}=0\ \text{on}\ \Gamma\}\,.$$

The variational formulation of the junction problem of two plates with a rigid hinge can be obtained by similarity with the previous one (see Section 3.1); it is given by

$$\text{Find } (\boldsymbol{u}; \underset{\sim}{\boldsymbol{u}}) \in W_{\text{Rig}}\,, \quad \text{such that } a[(\boldsymbol{u}; \underset{\sim}{\boldsymbol{u}}), (\boldsymbol{v}; \underset{\sim}{\boldsymbol{v}})] = l(\boldsymbol{v}; \underset{\sim}{\boldsymbol{v}}) \quad \forall (\boldsymbol{v}; \underset{\sim}{\boldsymbol{v}}) \in W_{\text{Rig}}\,, \tag{3.2.1}$$

where $a[(\cdot\,;\cdot\,), (\cdot\,;\cdot\,)]$ and $l(\cdot\,;\cdot\,)$ are bilinear and linear forms defined by (3.1.8) and (3.1.10).

THEOREM 3.2.1. Under the assumptions of Theorem 3.1.1, (3.2.1) has one and only one solution.

Proof. This proof is similar to that of Theorem 3.1.1. Briefly, we consider the following steps:

Step 1. The space W_{Rig} is a closed subspace of the space E defined by (3.1.12).

Step 2. Upon the space W_{Rig}, the semi-norm

$$|(\boldsymbol{v}; \underset{\sim}{\boldsymbol{v}})|_{W_{\text{Rig}}} = \Big(\int_S [e_{\alpha\beta}(\boldsymbol{v}) e_{\alpha\beta}(\boldsymbol{v}) + K_{\alpha\beta}(\boldsymbol{v}) K_{\alpha\beta}(\boldsymbol{v})]\, \mathrm{d}S \\ + \int_{\underset{\sim}{S}} [\underset{\sim}{e}_{\alpha\beta}(\underset{\sim}{\boldsymbol{v}}) \underset{\sim}{e}_{\alpha\beta}(\underset{\sim}{\boldsymbol{v}}) + \underset{\sim}{K}_{\alpha\beta}(\underset{\sim}{\boldsymbol{v}}) \underset{\sim}{K}_{\alpha\beta}(\underset{\sim}{\boldsymbol{v}})]\, \mathrm{d}\underset{\sim}{S} \Big)^{1/2} \tag{3.2.2}$$

is equivalent to the norm (3.1.13).

Step 3. Then, the bilinear form a$[(\cdot\,;\cdot\,), (\cdot\,;\cdot\,)]$ is continuous, symmetric and W_{Rig}-elliptic, and the linear form $l(\cdot\,;\cdot\,)$ is continuous on W_{Rig}. We conclude by using the Lax–Milgram theorem. □

3.3. *Study of the behaviour of an elastic hinge when $k \to \infty$*

The next theorem justifies the assertion of Remark 2.2.1.

THEOREM 3.3.1. Let $(\boldsymbol{u}^k; \underset{\sim}{\boldsymbol{u}}^k)$ be the solution of (3.1.7) and let $(\boldsymbol{u}; \boldsymbol{u})$ be the solution of (3.2.1). *Then $(\boldsymbol{u}^k; \underset{\sim}{\boldsymbol{u}}^k)$ is strongly convergent to $(\boldsymbol{u}, \underset{\sim}{\boldsymbol{u}})$ in W_{El}* when k goes to $+\infty$.

PROOF. It takes four steps.

Step 1. Weak convergence of $(\boldsymbol{u}^k; \underset{\sim}{\boldsymbol{u}}^k)$ in W_{El}:

By using the continuity of the linear form $l(\cdot\,;\cdot\,)$ on W_{El} and the W_{El}-ellipticity of the bilinear form

$$a_k[(\cdot\,;\cdot\,), (\cdot\,;\cdot\,)] = a[(\cdot\,;\cdot\,), (\cdot\,;\cdot\,)] + kb[(\cdot\,;\cdot\,), (\cdot\,;\cdot\,)]\,,$$

we obtain

$$\|(\boldsymbol{u}^k; \underset{\sim}{\boldsymbol{u}}^k)\|_{W_{\text{El}}} \leq \frac{\|l\|}{\alpha}\,,$$

as soon as $k \geq \alpha$ with $\alpha = \min\{Ee/(1-\nu^2), Ee^3/12(1-\nu^2), \underset{\sim}{E}\underset{\sim}{e}/(1-\underset{\sim}{\nu}^2), \underset{\sim}{E}\underset{\sim}{e}^3/12(1-\underset{\sim}{\nu}^2)\}$.

Since the sequence $(\boldsymbol{u}^k; \underset{\sim}{u}^k)$ is bounded in W_{El}, we can extract a subsequence, still noted $(\boldsymbol{u}^k; \underset{\sim}{u}^k)$ which is weakly convergent to $(\boldsymbol{u}^*; \underset{\sim}{u}^*)$ in W_{El}.

Step 2. $(\boldsymbol{u}^*; \underset{\sim}{u}^*) \in W_{\mathrm{Rig}}$.

By choosing $(\boldsymbol{v}; \underset{\sim}{v}) = (\boldsymbol{u}^k; \underset{\sim}{u}^k)$ in (3.1.7), we get

$$b[(\boldsymbol{u}^k; \underset{\sim}{u}^k), (\boldsymbol{u}^k; \underset{\sim}{u}^k)] \leq \frac{1}{k} \|l\| \, \|(\boldsymbol{u}_k; \underset{\sim}{u}_k)\|_{W_{\mathrm{El}}} \leq \frac{\|l\|^2}{k\alpha} .$$

The application

$$(\boldsymbol{u}^k; \underset{\sim}{u}^k) \to b[(\boldsymbol{u}^k; \underset{\sim}{u}^k), (\boldsymbol{u}^k; \underset{\sim}{u}^k)]$$

is convex and continuous upon $H^2(S) \times H^2(\underset{\sim}{S})$. Then it is lower weakly semicontinuous, so that for $k \to +\infty$, we obtain $b[(\boldsymbol{u}^*; \underset{\sim}{u}^*), (\boldsymbol{u}^*; \underset{\sim}{u}^*)] = 0$, i.e., $u^*_{3,n} = \underset{\sim}{u}^*_{3,\underset{\sim}{n}}$ on Γ which is the expected result.

Step 3. $(\boldsymbol{u}^*; \underset{\sim}{u}^*) = (\boldsymbol{u}; \underset{\sim}{u})$.

Since $W_{\mathrm{Rig}} \subset W_{\mathrm{El}}$, (3.1.7) implies

$$a[(\boldsymbol{u}^k; \underset{\sim}{u}^k), (\boldsymbol{v}; \underset{\sim}{v})] = l(\boldsymbol{v}; \underset{\sim}{v}) \quad \forall (\boldsymbol{v}; \underset{\sim}{v}) \in W_{\mathrm{Rig}} ,$$

so that for $k \to +\infty$

$$(\boldsymbol{u}^*, \underset{\sim}{u}^*) \in W_{\mathrm{Rig}} , \qquad a[(\boldsymbol{u}^*; \underset{\sim}{u}^*), (\boldsymbol{v}; \underset{\sim}{v})] = l(\boldsymbol{v}; \underset{\sim}{v}) \quad \forall (\boldsymbol{v}; \underset{\sim}{v}) \in W_{\mathrm{Rig}} .$$

Since this problem has $(\boldsymbol{u}; \underset{\sim}{u})$ as unique solution, we get the result.

Step 4. Strong convergence of $(\boldsymbol{u}^k, \underset{\sim}{u}^k)$ in W_{El}.

We have from Step 3 of the proof of Theorem 3.1.1

$$\begin{aligned} 0 &\leq C\|(\boldsymbol{u}; \underset{\sim}{u}) - (\boldsymbol{u}^k; \underset{\sim}{u}^k)\|^2_{W_{\mathrm{El}}} \\ &\leq a_k[(\boldsymbol{u}^k; \underset{\sim}{u}^k), (\boldsymbol{u}^k; \underset{\sim}{u}^k)] - 2a_k[(\boldsymbol{u}; \underset{\sim}{u}), (\boldsymbol{u}^k; \underset{\sim}{u}^k)] + a_k[(\boldsymbol{u}; \underset{\sim}{u}), (\boldsymbol{u}; \underset{\sim}{u})] . \end{aligned}$$

But, for the $(\boldsymbol{u}; \underset{\sim}{u})$ solution of the rigid problem (3.2.1), we have

$$a_k[(\boldsymbol{u}; \underset{\sim}{u}), (\boldsymbol{u}^k; \underset{\sim}{u}^k)] = a[(\boldsymbol{u}; \underset{\sim}{u}), (\boldsymbol{u}^k; \underset{\sim}{u}^k)] ,$$

so that the previous inequalities become

$$0 \leq C\|(\boldsymbol{u}; \underset{\sim}{u}) - (\boldsymbol{u}^k; \underset{\sim}{u}^k)\|^2_{W_{\mathrm{El}}} \leq l(\boldsymbol{u}^k; \underset{\sim}{u}^k) - 2a[(\boldsymbol{u}; \underset{\sim}{u}), (\boldsymbol{u}^k; \underset{\sim}{u}^k)] + l(\boldsymbol{u}; \underset{\sim}{u}) .$$

It remains to use the weak convergence of $(\boldsymbol{u}^k; \underset{\sim}{u}^k)$ to $(\boldsymbol{u}; \underset{\sim}{u})$ to prove the convergence to zero of the right hand member. This result implies the strong convergence of $(\boldsymbol{u}^k; \underset{\sim}{u}^k)$ to $(\boldsymbol{u}; \underset{\sim}{u})$. Since this limite is independent of the subsequence into consideration, the result is valid for the whole sequence $(\boldsymbol{u}^k; \underset{\sim}{u}^k)$. □

4. Approximation by conforming finite element methods

This paragraph is devoted to the approximation of (3.1.7) and (3.2.1) by conforming finite element methods. We consider two cases corresponding to an elastic hinge and to a rigid hinge.

4.1. *Approximation in case of an elastic hinge*

The approximation of the solution of (3.1.7) is realized by means of a conforming finite element method. Thus, we define a finite dimensional subspace

$$W^h_{\mathrm{El}} \subset W_{\mathrm{El}} \tag{4.1.1}$$

as follows:

$$W^h_{\mathrm{El}} = \{(\boldsymbol{w}_h; \underset{\sim}{\boldsymbol{w}}_h) \in (\boldsymbol{V}_h; \underset{\sim}{\boldsymbol{V}}_h) \mid \boldsymbol{w}_h(M) = \underset{\sim}{\boldsymbol{w}}_h(M)\ \ \forall M \in \Gamma\}\,, \tag{4.1.2}$$

with

$$\boldsymbol{V}_h = V_{h1} \times V_{h1} \times V_{h2}\,, \qquad \underset{\sim}{\boldsymbol{V}}_h = \underset{\sim}{V}_{h1} \times \underset{\sim}{V}_{h1} \times \underset{\sim}{V}_{h2}\,,$$

$$V_{h1} \subset V_1, V_{h2} \subset V_2\,, \qquad \underset{\sim}{V}_{h1} \subset H^1(\underset{\sim}{S}); \underset{\sim}{V}_{h2} \subset H^2(\underset{\sim}{S})\,.$$

The spaces V_{h1} and $\underset{\sim}{V}_{h1}$ are constructed from Hermite triangles of type (3′) (see Fig. 2), while the spaces V_{h2} and $\underset{\sim}{V}_{h2}$ are constructed from the $\mathscr{C}^1$-class reduced Hsieh–Clough–Tocher triangles (see Fig. 3).

Inclusion (4.1.1) implies that the following discrete problem associated to the continuous problem (3.1.7) has one and only one solution:

$$\begin{aligned}\text{Find } (\boldsymbol{u}^*_h; \underset{\sim}{\boldsymbol{u}}^*_h) \in W^h_{\mathrm{El}}\,, \quad \text{such that } & a[(\boldsymbol{u}^*_h; \underset{\sim}{\boldsymbol{u}}^*_h), (\boldsymbol{v}_h; \underset{\sim}{\boldsymbol{v}}_h)] + kb[(\boldsymbol{u}^*_h; \underset{\sim}{\boldsymbol{u}}^*_h), (\boldsymbol{v}_h; \underset{\sim}{\boldsymbol{v}}_h)] \\ &= l(\boldsymbol{v}_h; \underset{\sim}{\boldsymbol{v}}_h) \quad \forall (\boldsymbol{v}_h, \underset{\sim}{\boldsymbol{v}}_h) \in W^h_{\mathrm{El}}\,. \end{aligned} \tag{4.1.3}$$

But the exact computation of the integrals which appear in (4.1.3) is generally impossible. This makes the use of numerical integration techniques necessary. This leads to the definition

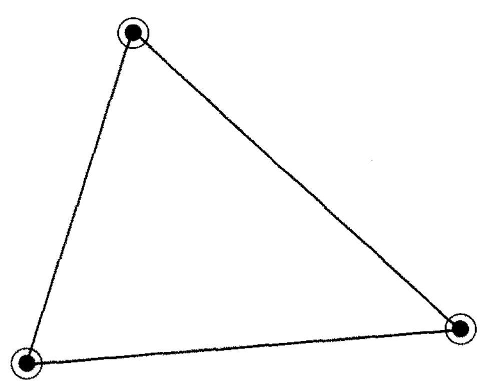

Fig. 2. Hermite triangle of type (3′) (see [11, p. 68]).

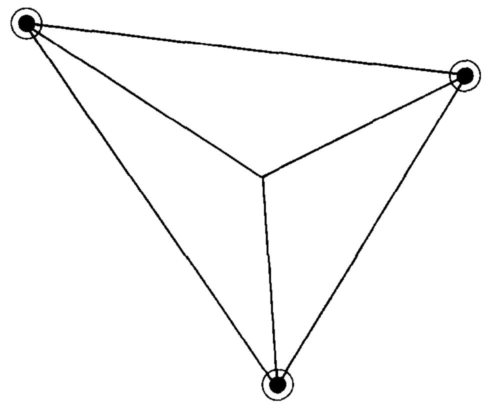

Fig. 3. Reduced HCT-triangle (see [11, p. 357]).

of a second discrete problem:

$$\text{Find } (\boldsymbol{u}_h; \underset{\sim}{u}_h) \in W^h_{\mathrm{El}}\,, \quad \text{such that } a_h[(\boldsymbol{u}_h; \underset{\sim}{u}_h), (\boldsymbol{v}_h; \underset{\sim}{v}_h)] + kb[(\boldsymbol{u}_h; \underset{\sim}{u}_h), (\boldsymbol{v}_h; \underset{\sim}{v}_h)] = l_h(\boldsymbol{v}_h; \underset{\sim}{v}_h) \quad \forall (\boldsymbol{v}_h, \underset{\sim}{v}_h) \in W^h_{\mathrm{El}}\,, \tag{4.1.4}$$

where the forms $a_h(\cdot\,,\cdot)$ and $l_h(\cdot)$ are deduced from forms $a(\cdot\,,\cdot)$ and $l(\cdot)$ through the use of appropriate numerical integration schemes. Moreover we will see in Section 4.3.2 that the bilinear form $b(\cdot\,,\cdot)$ can be computed exactly.

It remains to prove the existence, uniqueness and convergence of the solution $(\boldsymbol{u}_h; \underset{\sim}{u}_h)$ to the solution $(\boldsymbol{u}; \underset{\sim}{u})$ of (3.1.5). Such a study follows the lines of [12] and is detailed in [10].

For instance, when the boundaries ∂S_1 and $\partial \underset{\sim}{S}_1$ are unloaded and when the data and the solution $(\boldsymbol{u}; \underset{\sim}{u})$ of the continuous problem (3.1.7) are sufficiently smooth, then such methods allow to prove that there exist a constant C, independent of h, such that

$$\|(\boldsymbol{u}; \underset{\sim}{u}) - (\boldsymbol{u}_h; \underset{\sim}{u}_h)\|_E \leqslant Ch \tag{4.1.5}$$

as soon as the numerical integration schemes used to compute the integrals upon S and $\underset{\sim}{S}$ are exact for polynomials

(i) of degree 4 for the membrane terms (there exist such schemes involving 6 nodes per triangle)

(ii) of degree 2 for the bending terms upon each subtriangle of the HCT triangles (there exist such schemes involving 3 nodes).

When the boundaries ∂S_1 and $\partial \underset{\sim}{S}_1$ are loaded, we have to introduce some appropriate numerical integration technique for approximating the integrals along these boundaries. This study can be done as in [13] so that the estimate is still valid.

4.2. Approximation in case of a rigid hinge

The formulations are similar to those of Section 4.1, except for the definition of the finite dimensional subspace W^h_{Rig} which has to satisfy

$$W^h_{\mathrm{Rig}} \subset W_{\mathrm{Rig}}\,. \tag{4.2.1}$$

It is defined by

$$W^h_{\mathrm{Rig}} = \{(\boldsymbol{w}_h; \underset{\sim}{\boldsymbol{w}}_h) \in (\boldsymbol{V}_h; \underset{\sim}{\boldsymbol{V}}_h) \mid \boldsymbol{w}_h(M) = \underset{\sim}{\boldsymbol{w}}_h(M) \text{ and } w_{h3,n}(M) + \underset{\sim}{w}_{h3,\underset{\sim}{n}}(M) = 0 \ \forall M \in \Gamma\}, \tag{4.2.2}$$

so that the second discrete problem associated to the use of a numerical integration scheme can be stated as follows (compare with (4.1.4)):

$$\begin{aligned} &\text{Find } (\boldsymbol{u}_h; \underset{\sim}{\boldsymbol{u}}_h) \in W^h_{\mathrm{Rig}}, \quad \text{such that} \\ &a_h[(\boldsymbol{u}_h; \underset{\sim}{\boldsymbol{u}}_h), (\boldsymbol{v}_h; \underset{\sim}{\boldsymbol{v}}_h)] = l_h(\boldsymbol{v}_h; \underset{\sim}{\boldsymbol{v}}_h) \quad \forall(\boldsymbol{v}_h, \underset{\sim}{\boldsymbol{v}}_h) \in W^h_{\mathrm{Rig}}. \end{aligned} \tag{4.2.3}$$

As in Section 4.1, the methods developed in [10, 12, 13] would allow us to obtain an a priori estimate of type (4.1.5) as soon as the data, the solution and the numerical integration schemes are sufficiently regular.

REMARK 4.2.1. Of course, the solutions $(\boldsymbol{u}_h; \underset{\sim}{\boldsymbol{u}}_h)$ of (4.1.4) and (4.2.3) are different; in particular, the solution of (4.1.4) is depending on k.

4.3. *Implementation in case of an elastic hinge*

Upon each plate S and $\underset{\sim}{S}$ the implementation follows the usual lines, i.e., computation of local matrices, element by element, and assemblage into the global matrices as the computations proceed. In fact the only new part of such an implementation is related to the hinge. There are two new things to consider.

4.3.1. *Taking the condition $\boldsymbol{w}_h(M) = \underset{\sim}{\boldsymbol{w}}_h(M)$ $\forall M \in \Gamma$ into account*

This junction condition is an essential part of the definition of the space (4.1.2). By choosing the reference systems $(\boldsymbol{n}, \boldsymbol{t}, \boldsymbol{e}_3)$ and $(\underset{\sim}{\boldsymbol{n}}, \underset{\sim}{\boldsymbol{t}}, \underset{\sim}{\boldsymbol{e}}_3)$ along Γ, respectively attached to the plates S and $\underset{\sim}{S}$, the condition $\boldsymbol{w}_h(M) = \underset{\sim}{\boldsymbol{w}}_h(M)$ $\forall M \in \Gamma$, implies (see (2.2.7)):

$$\underset{\sim}{w}_{h\underset{\sim}{n}} = w_{hn} \cos\theta - w_{h3} \sin\theta, \quad \underset{\sim}{w}_{h\underset{\sim}{t}} = -w_{ht}, \quad \underset{\sim}{w}_{h3} = -w_{hn} \sin\theta - w_{h3} \cos\theta\,. \tag{4.3.1}$$

Moreover, the condition $\boldsymbol{w}_h(M) = \underset{\sim}{\boldsymbol{w}}_h(M)$ $\forall M \in \Gamma$ implies $\boldsymbol{w}_{h,t}(M) = -\underset{\sim}{\boldsymbol{w}}_{h,\underset{\sim}{t}}(M)$ $\forall M \in \Gamma$. Thus, it follows from (4.3.1) that

$$\underset{\sim}{w}_{h\underset{\sim}{n},\underset{\sim}{t}} = -w_{hn,t} \cos\theta + w_{h3,t} \sin\theta, \quad \underset{\sim}{w}_{h\underset{\sim}{t},\underset{\sim}{t}} = w_{ht,t}, \quad \underset{\sim}{w}_{h3,\underset{\sim}{t}} = w_{hn,t} \sin\theta + w_{h3,t} \cos\theta\,. \tag{4.3.2}$$

The restrictions of these functions w_{hn}, w_{ht}, w_{h3}, $\underset{\sim}{w}_{h\underset{\sim}{n}}$, $\underset{\sim}{w}_{h\underset{\sim}{t}}$ and $\underset{\sim}{w}_{h3}$ to the hinge Γ are polynomials of order 3 in one variable upon each side a_1a_2 located on Γ. Then, to satisfy (4.3.1) and (4.3.2) at any point of Γ, it suffices to satisfy them at any vertex located on Γ. Thus the main unknowns of the problem can be chosen as the values of

$$u_{hn}\,,\quad u_{ht}\,,\quad u_{h3}\,,\quad u_{hn,n}\,,\quad u_{hn,t}\,,\quad u_{ht,n}\,,\quad u_{ht,t}\,,\quad u_{h3,n}\,,\quad u_{h3,t}\,,\quad \underset{\sim}{u}_{h\underset{\sim}{n},\underset{\sim}{n}}\,,$$
$$\underset{\sim}{u}_{h\underset{\sim}{t},\underset{\sim}{n}}\,,\quad \underset{\sim}{u}_{h3,\underset{\sim}{n}}\,, \tag{4.3.3}$$

at any vertex of the mesh located on Γ. Of course (4.3.1) and (4.3.2) are symmetrical in w and $\underset{\sim}{w}$ so that we could permute the roles of u and $\underset{\sim}{u}$ in (4.3.3).

4.3.2. Exact computation of $b[(\boldsymbol{u}_h;\underset{\sim}{\boldsymbol{u}}_h),(\boldsymbol{v}_h;\underset{\sim}{\boldsymbol{v}}_h)]$

According to (3.1.9), we have

$$b[(\boldsymbol{u}_h;\underset{\sim}{\boldsymbol{u}}_h);(\boldsymbol{v}_h;\underset{\sim}{\boldsymbol{v}}_h)] = \int_\Gamma (u_{h3,n} + \underset{\sim}{u}_{h3,\underset{\sim}{n}})(v_{h3,n} + \underset{\sim}{v}_{h3,\underset{\sim}{n}})\,\mathrm{d}\gamma\,. \tag{4.3.4}$$

By definition of the reduced HCT-triangle we obtain

$$u_{h3,n}(M) = \lambda u_{h3,n}(a_1) + (1-\lambda)u_{h3,n}(a_2) \tag{4.3.5}$$

for any point M belonging to a side a_1a_2 of a triangle, this side being located upon the hinge Γ.

Of course, we have similar relations for $\underset{\sim}{u}_{h3,\underset{\sim}{n}}$, $v_{h3,n}$ and $\underset{\sim}{v}_{h3,\underset{\sim}{n}}$. Thus, it is easy to check that

$$\begin{aligned}
&b[(\boldsymbol{u}_h;\underset{\sim}{\boldsymbol{u}}_h);(\boldsymbol{v}_h;\underset{\sim}{\boldsymbol{v}}_h)]\\
&= \sum_{[a_1,a_2]\in\Gamma} \{\tfrac{1}{3}[u_{h3,n}(a_1) - \underset{\sim}{u}_{h3,\underset{\sim}{n}}(a_1)][v_{h3,n}(a_1) - \underset{\sim}{v}_{h3,\underset{\sim}{n}}(a_1)]\\
&\qquad + \tfrac{1}{6}[u_{h3,n}(a_1) - \underset{\sim}{u}_{h3,\underset{\sim}{n}}(a_1)][v_{h3,n}(a_2) - \underset{\sim}{v}_{h3,\underset{\sim}{n}}(a_2)]\\
&\qquad + \tfrac{1}{6}[u_{h3,n}(a_2) - \underset{\sim}{u}_{h3,\underset{\sim}{n}}(a_2)][v_{h3,n}(a_1) - \underset{\sim}{v}_{h3,\underset{\sim}{n}}(a_1)]\\
&\qquad + \tfrac{1}{3}[u_{h3,n}(a_2) - \underset{\sim}{u}_{h3,\underset{\sim}{n}}(a_2)][v_{h3,n}(a_2) - \underset{\sim}{v}_{h3,\underset{\sim}{n}}(a_2)]\}\,.
\end{aligned} \tag{4.3.6}$$

These contributions are easy to assemble in the global rigidity matrix.

4.4. Implementation in case of a rigid hinge

The main differences with the previous case are

(i) the additional condition $w_{h3,n}(M) + \underset{\sim}{w}_{h3,\underset{\sim}{n}}(M) = 0\ \forall M\in\Gamma$ which appears in the definition of the space W^h_{Rig} (4.2.2),

(ii) the absence of term $b[\cdot\,;\cdot]$ in (4.2.3).

The comparison with Section 4.3.1 shows immediately that conditions (4.3.1) and (4.3.2) are still valid and that they have to be complemented by the additional relation $w_{h3,n}(M) = -\underset{\sim}{w}_{h3,\underset{\sim}{n}}(M)\ \forall M\in\Gamma$. Thus, we have the following relations to satisfy at any point $M\in\Gamma$:

$$\begin{aligned}
&\underset{\sim}{w}_{h\underset{\sim}{n}} = w_{hn}\cos\theta - w_{h3}\sin\theta\,, && \underset{\sim}{w}_{ht} = -w_{ht}\,, && \underset{\sim}{w}_{h3} = -w_{hn}\sin\theta - w_{h3}\cos\theta\,,\\
&\underset{\sim}{w}_{h\underset{\sim}{n},\underset{\sim}{t}} = -w_{hn,t}\cos\theta + w_{h3,t}\sin\theta\,, && \underset{\sim}{w}_{h\underset{\sim}{t},\underset{\sim}{t}} = w_{ht,t}\,, && \underset{\sim}{w}_{h3,\underset{\sim}{t}} = w_{hn,t}\sin\theta + w_{h3,t}\cos\theta\,,\\
&\underset{\sim}{w}_{h3,\underset{\sim}{n}} = -w_{h3,n}\,.
\end{aligned} \tag{4.4.1}$$

Thus similar arguments to those used in Section 4.3 prove that we can choose the following set of main unknowns:

$$u_{hn}\,,\quad u_{ht}\,,\quad u_{h3}\,,\quad u_{hn,n}\,,\quad u_{hn,t}\,,\quad u_{ht,n}\,,\quad u_{ht,t}\,,\quad u_{h3,n}\,,\quad u_{h3,t}\,,\quad \underset{\sim}{u}_{h\underset{\sim}{n},\underset{\sim}{n}}\,,\quad \underset{\sim}{u}_{h\underset{\sim}{t},\underset{\sim}{n}}\,, \tag{4.4.2}$$

at any vertex of the mesh located on Γ. In particular, we have used that the restrictions of $w_{h3,n}$ and $\underset{\sim}{w}_{h3,\underset{\sim}{n}}$ to Γ are locally polynomials of degree one.

5. Numerical examples

We have considered the three following examples which have been implemented in MODULEF (see [14]).

5.1. Example of a folded cantilever plate with rigid hinge, subjected to a line load at its tip

This example is extracted from [2] and [15, test no. A-24].

According to Fig. 4, we consider a rigid junction of two plates: the first one is clamped along the side aa' while the second one is loaded along the side cc' by a line density of forces

$$P_Z = -1\ \mathrm{lb/in}\,.$$

For this study we have used the mesh shown in Fig. 5. Upon this figure we represent the deformed configuration of the cantilever plate which is in good agreement with the results reported in [15].

In particular, we find $Z_A = -0.000837274$ in and $Z_B = -0.000837166$ in.

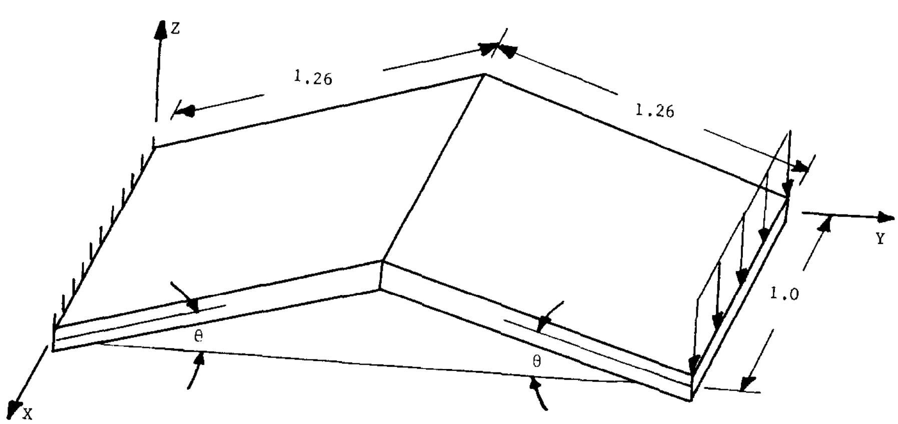

Fig. 4. The folded cantilever plate. $e = 0.124$ in, $\theta = 30°$, $E = 3 \cdot 10^7$ psi, $\nu = 0$.

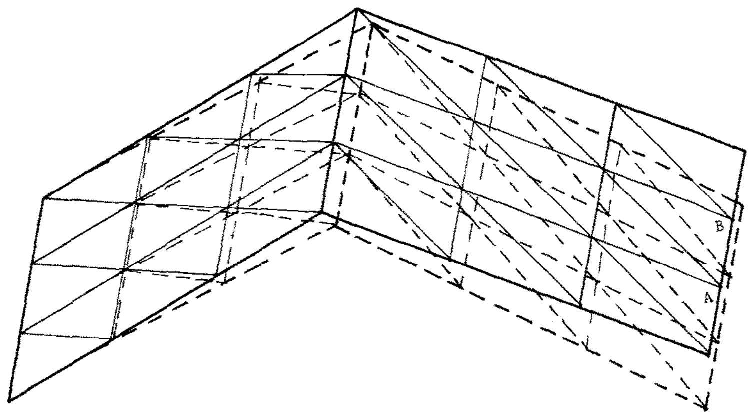

Fig. 5. The cantilever before loading (——) and after loading (- - -) for a rigid hinge.

5.2. Example of a multifolded plate with rigid hinges

This example was previously considered in [16, 17]. With notations of Fig. 6, the structure is clamped along the side $a'f'$ and loaded along the hinges by two types of line densities:

$$P_Z^1 = 1.22\ \text{lb/in along the hinges } bb' \text{ and } ee'\ ,$$

$$P_Z^2 = 1.00\ \text{lb/in along the hinges } cc' \text{ and } dd'\ .$$

For this study we have used the mesh shown in Fig. 7.

The experimental results and the analytical solution are extracted from [16]. They are included with our numerical results in Table 1.

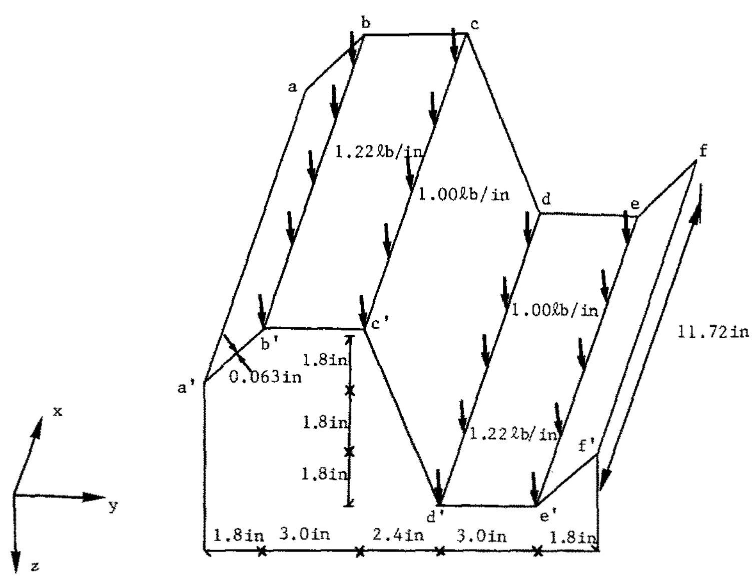

Fig. 6. Multifolded plate ($E = 10.6 \cdot 10^6$ psi (aluminium), $\nu = 0.33$).

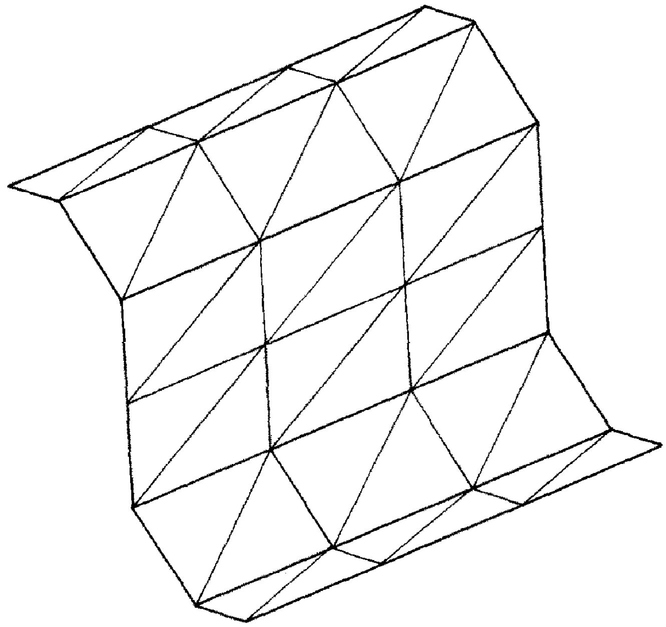

Fig. 7. Mesh in use.

Table 1
Vertical displacement of points a to f

	u_Z (in)					
Points	a	b	c	d	e	f
Experimental	—	0.0058	0.0013	0.0012	0.0063	—
Analytical	0.0136	0.0080	0.0008	0.0008	0.0080	0.0136
Numerical	0.0134	0.0070	0.0008	0.0008	0.0060	0.0122

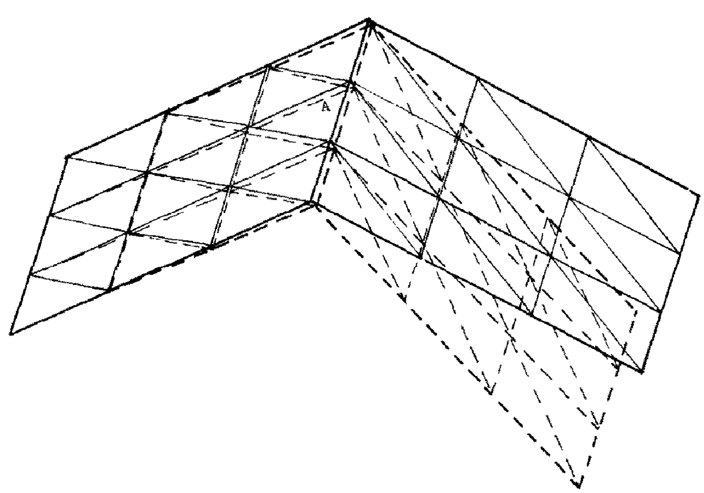

Fig. 8. The folded cantilever before loading (——) and after loading (- - -) for an elastic hinge. $k = 10^4$ lb.

5.3. Example of a folded cantilever plate with elastic hinge subjected to a line load at its tip

The data are identical to those of the first example except that now the hinge is supposed to be elastic. Figures 8 and 9 present the deformed configuration when $k = 10^4$ lb and $k = 10^3$ lb.

Finally, Fig. 10 shows the jump of the rotation $(\boldsymbol{\Omega} - \underset{\sim}{\boldsymbol{\Omega}}) \cdot \boldsymbol{t} = -(u_{3,n} + \underset{\sim}{u}_{3,\underset{\sim}{n}})$ at point $A \in \Gamma$ (see Figs. 8 and 9). We can check that the hinge behaves

(i) as a knee-joint when the coefficient k is small,

(ii) as a rigid hinge when the coefficient k is very large.

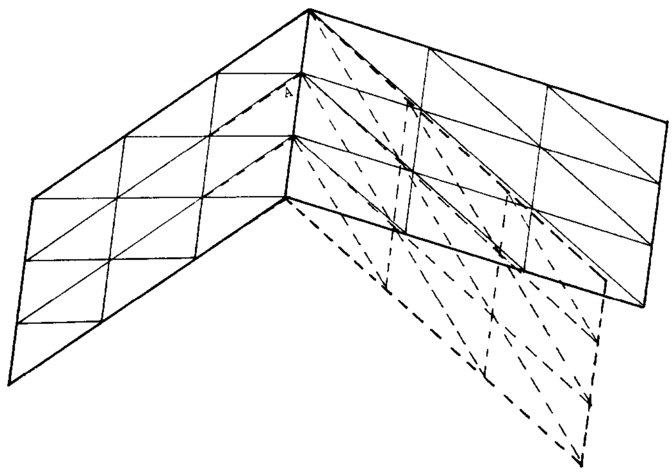

Fig. 9. The folded cantilever before loading (——) and after loading (---) for an elastic hinge. $k = 10^3$ lb.

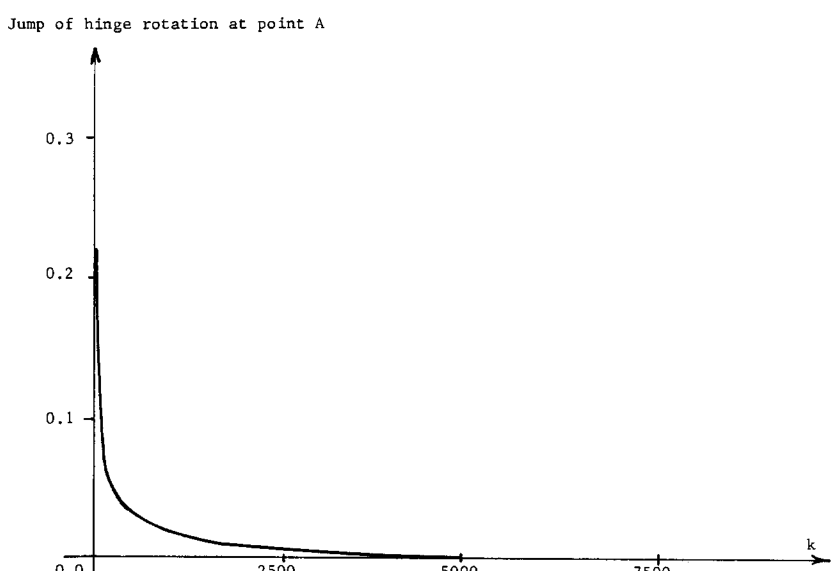

Fig. 10. Jump of the hinge rotation at point A as a function of coefficient k.

6. Conclusion

This study gives a precise variational formulation of the junction problem of two plates by using appropriate functional spaces. From this formulation, we have approximated the solution by conforming finite element methods which are easy to implement.

By using the same ideas we are extending these results to the junction of two shells having general shapes.

Acknowledgement

The authors are indebted to Pr. G. Duvaut for suggesting this approach and for several useful discussions. They also acknowledge Asulab S.A. for partly supporting this study.

References

[1] E.H. Baker, L. Kovalevsky, F.L. Rish, Structural Analysis of Shells (Krieger, Huntington, NY, 1981).
[2] K.J. Bathe, L.W. Ho, Some results in the analysis of thin shell structures, in: W. Wunderlich, E. Stein and K.-J. Bathe eds., Nonlinear Finite Element Analysis in Structural Mechanics (Springer, Berlin, 1981) 122–150.
[3] K.J. Bathe, Finite Element Procedures in Engineering Analysis (Prentice-Hall, Englewood Cliffs, NJ, 1982).
[4] P.G. Ciarlet, Modelling and numerical analysis of junctions between elastic structures, in: J. McKenna and R. Temam, eds. Proc. of the First Internat. Conf. on Industrial and Applied Mathematics, Paris, 1987 (SIAM, Philadelphia, 1988) 62–74.
[5] P.G. Ciarlet, H. Le Dret, R. Nzengwa, Modélisation de la jonction entre un corps élastique tridimensionnel et une plaque, C.R. Acad. Sci. Paris 305 (I) (1987) 55–58.
[6] M. Aufranc, Etudes numériques de raccords de structures élastiques de dimensions différentes, Rapports de Recherche INRIA 781 (Février, 1988).
[7] H. Le Dret, Modelling of a folded plate, publications du laboratoire d'analyse numérique de l'Université Pierre et Marie Curie R87017 (1987) Asymptotic Analysis, to appear.
[8] H. Le Dret, Folded plates revisited, Publications du laboratoire d'analyse numérique de l'Université Pierre et Marie Curie R87032 (1987) Asymptotic Analysis, to appear.
[9] P. Germain, Cours de Mécanique (Ecole Polytechnique, 1979).
[10] S. Fayolle, Sur l'analyse numérique de raccords de poutres et de plaques, Thèse de 3ème cycle, Université Pierre et Marie Curie—Paris VI (1987).
[11] P.G. Ciarlet, The Finite Element Method for Elliptic Problems (North-Holland, Amsterdam, 1978).
[12] M. Bernadou, Convergence of conforming finite element methods for general shell problems, Internat. J. Engrg. Sci. 18 (1980) 249–276.
[13] M. Bernadou, Méthodes numériques, in: R. Dautray and J.L. Lions, eds., Analyse Mathématique et Calcul Numérique pour les Sciences et les Techniques Tome 2 (Masson, Paris, 1985) 703–910.
[14] M. Bernadou, P.L. George, A. Hassim, P. Joly, P. Laug, A. Perronnet, E. Saltel, D. Steer, G. Vanderborck, M. Vidrascu, Modulef, A Modular Finite Element Library (INRIA, Rocquencourt, 1986).
[15] ADINA (Automatic Dynamic Incremental Nonlinear Analysis), System verification manual, Report, AE 83-5 (ADINA Engineering, Inc. Watertown, 1983).
[16] A.C. Scordelis, E.L. Croy, I.R. Stubbs, Experimental and analytical study of a folded plate, ASCE J. Struct, Div. 87, ST8 (1961) 139–160.
[17] J.L. Meek, H.S. Tan, A faceted shell element with Loof nodes, Internat, J. Numer. Methods Engrg. 23 (1986) 49–67.